

MULTI-SCALE CORRELATION FUNCTIONS

M. E. Veysoglu and J. A. Kong

- 1. Introduction**
 - 2. Random Medium Model**
 - 3. Computation of Correlation Functions**
 - 3.1 Overview
 - 3.2 Basic Formulation
 - 3.3 Sparse Distribution of Particles
 - 3.4 Dense Distribution of Particles
 - 4. Summary and Conclusions**
 - 5. Appendix**
- References**

1. Introduction

Random medium models have been widely used to study electromagnetic and acoustic scattering properties of inhomogeneous geophysical media and turbulent atmosphere [1–9]. In these models, the permittivity is assumed to be a random function of space variables and spatial correlation functions are employed to describe the two point statistics of the permittivity fluctuations.

The purpose of this study is to investigate in detail the statistical description of a random medium and how it relates to the scattering properties of the random medium. The main focus of the study is on the correlation function since this function reflects important physical properties of the medium and plays a central role in scattering calculations. To be rigorous, a specific physical model is considered which consists of a collection of spheres with a given size distribution, and the computation of the correlation function is carried out for this well-defined configuration. It is very important to consider the size distribution of scatterers since power scattered from a particle varies rapidly

with the size. In fact, in the Rayleigh limit, the scattering cross section of a spherical particle is proportional to the sixth power of the radius which results in significant scattering from larger particles even if their number density is small. An accurate correlation function should reflect this effect.

To determine the correlation function, a novel technique is used: The scattering problem is first solved by the continuous random medium model leaving the correlation function as unknown. The scattering problem is then solved by the discrete scatterer model which requires the specification of shapes and distributions of the scatterers but not the correlation function. Finally, the results from two approaches are equated to obtain an equation for the correlation function. The solution of this equation is facilitated by treating the weak scattering case and employing the Born approximation to solve for the correlation function. However, the result is valid in general since the correlation function depends only on the geometric organization of particles and is independent of their scattering properties. In other words, if the correlation function can be uniquely determined in the weak scattering limit, it must be the correct solution for all scattering conditions since it is independent of such conditions. Sparse and dense distribution of particles are considered separately. For densely distributed particles, pair distribution functions [10–11] are introduced and the correlation functions are related to them. Various physical configurations are investigated by changing the size and fractional volume of the particles. The implications of multi-scale correlation functions are discussed.

The chapter consists of four sections. Following this introductory section, the random medium model is reviewed and the role of the correlation function is explained. In section 3, a review of previous results for single-scale correlation functions is given and the new computation technique is discussed for different physical configurations. Numerical results are presented for both single-scale and multi-scale correlation functions. Furthermore a unique relation between the size distribution of particles and the correlation function is established for sparsely distributed media which results in an explicit formula to determine the size distribution from the correlation function. In the final section, implications of the new results are discussed and conclusions are given.

2. Random Medium Model

A random medium is a mathematical model of a structurally complex medium. It consists of an ensemble of media and a probability distribution over the members of the ensemble. The random medium model represents a given medium well if each member of the ensemble is similar to it, or if the mean of the random medium is close to the given medium with small variance [12]. For instance, for electromagnetic propagation studies, the permittivity is assumed to be a random function of space variables which model three dimensional variations of permittivity fluctuations. In order to represent wave propagation in the medium, a random wave is considered which is a family of waves, one in each medium of the ensemble. The mean of the random wave, and its other statistics provide information about the wave in the given complex medium [12].

In random medium models, correlation functions play a significant role in propagation and scattering calculations. To demonstrate the importance of correlation functions, we will consider a random medium with strong permittivity fluctuations and apply strong fluctuation theory [13]; [14] to calculate scattered fields from the medium:

Consider a medium with permittivity $\epsilon(\vec{r})$ which is a random function of position. The vector wave equation for this medium is

$$\nabla \times \nabla \times \overline{E}(\vec{r}) - k_o^2 \frac{\epsilon(\vec{r})}{\epsilon_o} \overline{E}(\vec{r}) = 0 \quad (1)$$

where $k_o = \omega \sqrt{\mu_o \epsilon_o}$ is the free-space wavenumber. To determine the effective permittivity of the random medium under the strong fluctuation theory, a deterministic permittivity ϵ_g is introduced in both sides of this equation to get

$$\nabla \times \nabla \times \overline{E}(\vec{r}) - k_o^2 \frac{\epsilon_g}{\epsilon_o} \overline{E}(\vec{r}) = k_o^2 \left(\frac{\epsilon(\vec{r}) - \epsilon_g}{\epsilon_o} \right) \overline{E}(\vec{r}) \quad (2)$$

The permittivity ϵ_g has physical significance because in the low frequency limit, the effective permittivity can be well approximated by this quantity [8]. The effective permittivity in turn is one of the most important parameters in random medium models since the propagation of the mean field inside the random medium is solely determined by the effective permittivity. In fact, the mean field satisfies the wave

equation in a homogeneous medium with the given effective permittivity which implies that the attenuation of the mean field is described by the imaginary part of the effective permittivity.

If $\overline{\overline{G}}_g(\vec{r}, \vec{r}')$ is the dyadic Green's function that satisfies the vector wave equation with wavenumber $k_g = \omega\sqrt{\mu_o\epsilon_g}$, then

$$\nabla \times \nabla \times \overline{\overline{G}}_g(\vec{r}, \vec{r}') - k_g^2 \overline{\overline{G}}_g(\vec{r}, \vec{r}') = \overline{\overline{I}}\delta(\vec{r} - \vec{r}') \quad (3)$$

and

$$\overline{E}(\vec{r}) = \overline{E}_o(\vec{r}) + k_o^2 \int d\vec{r}' \overline{\overline{G}}_g(\vec{r}, \vec{r}') \frac{\epsilon(\vec{r}') - \epsilon_g}{\epsilon_o} \cdot \overline{E}(\vec{r}') \quad (4)$$

where $\overline{E}_o(\vec{r})$ is the field that satisfies the homogeneous wave equation with wavenumber k_g .

When the dyadic Green's function is decomposed into its principal value plus the singularity term for a spherical exclusion volume, it takes the following form:

$$\overline{\overline{G}}_g(\vec{r}, \vec{r}') = PV\overline{\overline{G}}_g(\vec{r}, \vec{r}') - \frac{\overline{\overline{I}}}{3k_g^2} \delta(\vec{r} - \vec{r}') \quad (5)$$

Substituting this into (4) gives

$$\overline{F}(\vec{r}) = \overline{E}_o(\vec{r}) + k_o^2 \int d\vec{r}' PV\overline{\overline{G}}_g(\vec{r}, \vec{r}') \xi(\vec{r}') \overline{F}(\vec{r}') \quad (6)$$

where

$$\overline{F}(\vec{r}) = \frac{\epsilon(\vec{r}) + 2\epsilon_g}{3\epsilon_g} \overline{E}(\vec{r}) \quad (7)$$

$$\xi(\vec{r}) = 3 \frac{\epsilon_g}{\epsilon_o} \left(\frac{\epsilon(\vec{r}) - \epsilon_g}{\epsilon(\vec{r}) + 2\epsilon_g} \right) \quad (8)$$

In these equations, $\overline{F}(\vec{r})$ and $\overline{E}(\vec{r})$ play the roles of external and internal fields, respectively.

Upon applying the bilocal approximation [8] to (6), an integral equation for the mean external field is obtained as

$$\langle \bar{F}(\bar{r}) \rangle = \bar{E}_o(\bar{r}) + k_o^2 \int d\bar{r}' \int d\bar{r}'' PV \bar{G}_g(\bar{r}, \bar{r}') \cdot \bar{\xi}_{eff}(\bar{r}', \bar{r}'') \cdot \langle \bar{F}(\bar{r}'') \rangle \quad (9)$$

with

$$\bar{\xi}_{eff}(\bar{r}', \bar{r}'') = k_o^2 PV \bar{G}_g(\bar{r}', \bar{r}'') C_\xi(|\bar{r}' - \bar{r}''|) \quad (10)$$

where

$$C_\xi(|\bar{r}' - \bar{r}''|) = \langle \xi(\bar{r}') \xi(\bar{r}'') \rangle \quad (11)$$

is the spherically symmetric correlation function of $\xi(\bar{r})$ where ϵ_g is chosen such that $\langle \xi(\bar{r}) \rangle = 0$ [13]. It is seen that the correlation function plays a central role in the propagation calculations. Furthermore, the effective permittivity under bilocal approximation is given as [8]

$$\epsilon_{eff} = \epsilon_g + \epsilon_o \frac{2}{3} k_o^2 \int_0^\infty dr r C_\xi(r) + i \frac{2}{3} k_o^2 k_g \epsilon_o \int_0^\infty dr r^2 C_\xi(r) \quad (12)$$

which demonstrates the importance of the correlation function. Further considerations of propagation in random media can be found in [15–17]. In the following section we discuss the computation of different correlation functions and their implications.

3. Computation of Correlation Functions

In the literature, several correlation functions have been derived and used for different physical configurations. Debye calculated a correlation function of exponential form for a medium which has scatterers of arbitrary shape and size [18]. When scatterers are of spherical shape, simple expressions for the correlation functions have been obtained for penetrable scatterers [19]. In addition, Hole-correction and Percus-Yevick pair distribution functions have been used to describe the statistics of impenetrable spheres [20–21].

However, in random medium models, much of the correlation functions used thus far have been assumed to be exponential [18; 22–23]. This is because the exponential correlation function is simple in

form and has been considered to be a reasonable approximation. Also, simple physical arguments have been used to obtain a correlation function for the random medium model [24–25]. However, to be rigorous in the modeling, the random medium should first be described in terms of the shape and size of the scatterers. The correlation function can then be derived and used in the random medium model. This approach gives a direct relationship between the physical configuration and the results obtained from the random medium model.

3.1 Overview

Consider the configuration shown in the Figure 1. The medium is described by a random permittivity function $\epsilon(\vec{r})$. The correlation function for this medium can be defined in terms of the permittivity function as follows

$$C(\vec{r} - \vec{r}') = \langle [\epsilon(\vec{r}) - \langle \epsilon(\vec{r}) \rangle][\epsilon(\vec{r}') - \langle \epsilon(\vec{r}') \rangle]^* \rangle \quad (13)$$

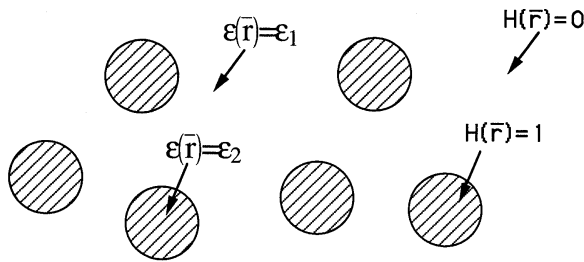


Figure 1. Problem Configuration.

For the configuration considered, $\langle \epsilon(\vec{r}) \rangle$ is independent of \vec{r} , and the correlation function depends on the difference vector $\vec{r} - \vec{r}'$. A random medium with these properties is called homogeneous [1].

The permittivity function can be expressed in terms of a new function $H(\vec{r})$ which takes the value 1 within the scatterer and 0 elsewhere:

$$\epsilon(\vec{r}') = (\epsilon_2 - \epsilon_1)H(\vec{r}') + \epsilon_1 \tag{14}$$

By substituting this expression in the definition of the correlation function above and simplifying, we obtain a new expression for the correlation function

$$C(\vec{r}) = |\epsilon_1 - \epsilon_2|^2 \langle H(\vec{r}')H(\vec{r}' + \vec{r}) \rangle - f^2 \tag{15}$$

where f is the fractional volume of the scatterer (medium 2). Here, the term within the angular brackets deserves special attention because once this function is determined the correlation function can be simply calculated. Let

$$P_{22}(\vec{r}) = \langle H(\vec{r}')H(\vec{r}' + \vec{r}) \rangle \tag{16}$$

It can be shown that $P_{22}(\vec{r})$ is the probability that both ends of a rod of length $r = |\vec{r}|$ which lies along \vec{r} is located in medium 2 (Figure 2). For an isotropic random medium, $P_{22}(\vec{r})$ is a function of r only.

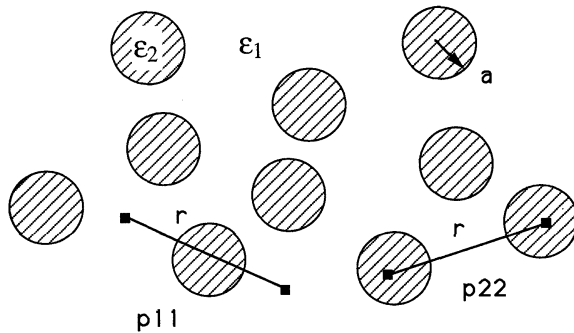


Figure 2. Illustrations for $P_{11}(r)$ and $P_{22}(r)$.

At this point, we note that $P_{22}(\vec{r})$ is in a sense more fundamental than the correlation function as defined in Equation (13) because definitions of correlation functions may vary for different applications. In fact we have seen in Section 2 that under strong fluctuation theory it is more convenient to define a correlation function in terms of $\xi(\vec{r})$ rather than $\epsilon(\vec{r})$. In either case however, the correlation function can be expressed in terms of $P_{22}(\vec{r})$ which indicates the significance of this probability function.

A similar expression for the correlation function can be obtained in terms of $P_{11}(r)$, the probability that both ends of the rod is within medium 1 (the background medium). Thus, the correlation function can be computed by either calculating $P_{11}(r)$ or $P_{22}(r)$.

$$C(r) = |\epsilon_1 - \epsilon_2|^2 (P_{22}(r) - f^2) \quad (17)$$

$$= |\epsilon_1 - \epsilon_2|^2 (P_{11}(r) - (1 - f)^2) \quad (18)$$

The normalized correlation function, which can be used in the calculation of effective permittivity and backscattering coefficients can then be defined as

$$R(r) = \frac{C(r)}{C(0)} = \frac{P_{22}(r) - f^2}{f - f^2} \quad (19)$$

$$= \frac{P_{11}(r) - (1 - f)^2}{(1 - f) - (1 - f)^2} \quad (20)$$

These are general definitions of the correlation and probability functions we will use in the subsequent sections of the chapter.

3.1.a Impenetrable model

In the case of impenetrable spheres, where the spheres cannot overlap with each other, it is convenient to calculate the correlation function by considering $P_{22}(r)$ which breaks down into two components: a self term and a cross term. The self term arises from the case in which both ends of the rod is contained within one scatterer and the cross term arises when the ends of the rod are in different scatterers. These two terms can be evaluated giving the following form for the probability function:

$$P_{22}(r) = f \left[1 - \frac{3r}{4a} + \frac{1}{16} \left(\frac{r}{a} \right)^3 \right] + f^2 \int_{V_2} d^3 r_1 \int_{V_1} d^3 r_2 g(|\bar{r}_2 - \bar{r}_1|) / \left(\frac{4}{3} \pi a^3 \right)^2 \quad (21)$$

where a is the radius of the spherical scatterer [21]. The derivation of this result will be given in the following section where it will also be generalized to multi-scale correlation functions.

It is interesting to see that the self term is proportional to the common volume between two intersecting spheres of radius a which are separated by a distance r . In other words, the probability that both ends of a given rod of length r is contained within one scatterer is proportional to the common volume between a sphere and its replica which is displaced from the center of the original sphere by a distance r . At this point, it is important to note that the medium under consideration consists of impenetrable spheres; the discussion of intersecting spheres is an abstract geometrical construction to explain the form of the self term.

The cross term, on the other hand, can be expressed in terms of a double volume integral over spheres located at $r(V1)$ and at the origin ($V2$). This term will be shown to be proportional to the convolution of the self term and the function $g(\vec{r}) \cdot g(|\vec{r}_2 - \vec{r}_1|)$ is the pair distribution function [10–11] which gives the probabilistic distribution of the scatterers in space for any given fractional volume. Depending on the type of pair distribution used, various correlation functions can be obtained. Shown in the Figure 3 is the Percus-Yevick pair distribution function for various fractional volumes [8].

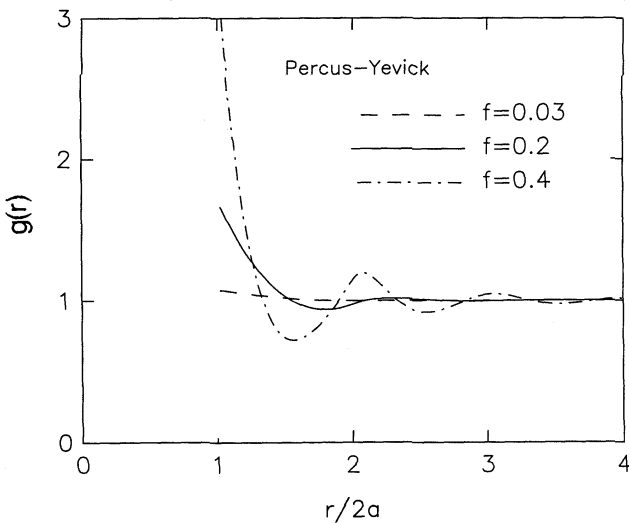


Figure 3. Percus-Yevick pair distribution function.

We note that at high fractional volume there is oscillation due to the crowding of the spheres to form a tight lattice. At low fractional volume, the pair distribution function is nearly flat since the spheres are far apart and almost independent of each other. In all cases, the pair distribution function is zero for r less than the diameter of the spheres since the spheres are impenetrable. For low fractional volume, a good approximation to the Percus-Yevick pair distribution function is the Hole-correction approximation [20–21]. The correlation function under this approximation can be carried out analytically by evaluating Equation (21) with the Hole-correction pair distribution function and using Equation (17). The result is given as

$$\begin{aligned}
 C(r) &= \Delta \left\{ f \left[1 - \frac{3}{4} \left(\frac{r}{a} \right) + \frac{1}{16} \left(\frac{r}{a} \right)^3 \right] + f^2 \left[\frac{9}{16} \left[\frac{1}{1260} \left(\frac{r}{a} \right)^6 \right. \right. \right. \\
 &\quad \left. \left. \left. - \frac{1}{10} \left(\frac{r}{a} \right)^4 + \frac{1}{3} \left(\frac{r}{a} \right)^3 \right] - 1 \right] \right\}, r < 2a \\
 &= \Delta \left\{ f^2 \left[\frac{9}{16} \left[-\frac{1}{1260} \left(\frac{r}{a} \right)^6 + \frac{1}{10} \left(\frac{r}{a} \right)^4 - \frac{5}{9} \left(\frac{r}{a} \right)^3 \right. \right. \right. \\
 &\quad \left. \left. \left. + \frac{32}{5} \left(\frac{r}{a} \right) - \frac{128}{9} + \frac{256}{35} \frac{a}{r} \right] \right] \right\}, \quad 2a \leq r < 4a \\
 &= 0, \quad 4a \leq r
 \end{aligned} \tag{22}$$

where $\Delta = |\epsilon_1 - \epsilon_2|^2$. The correlation function in the Percus-Yevick model can also be carried out analytically; however, the expressions become tedious and numerical evaluation is much simpler to use. This is done by reducing the six-fold integral in Equation (21) into a single integral which can easily be integrated numerically. Comparison of the normalized correlation functions obtained from the Percus-Yevick and Hole-correction pair distribution functions show good agreement for small fractional volume as seen in Figure 4.

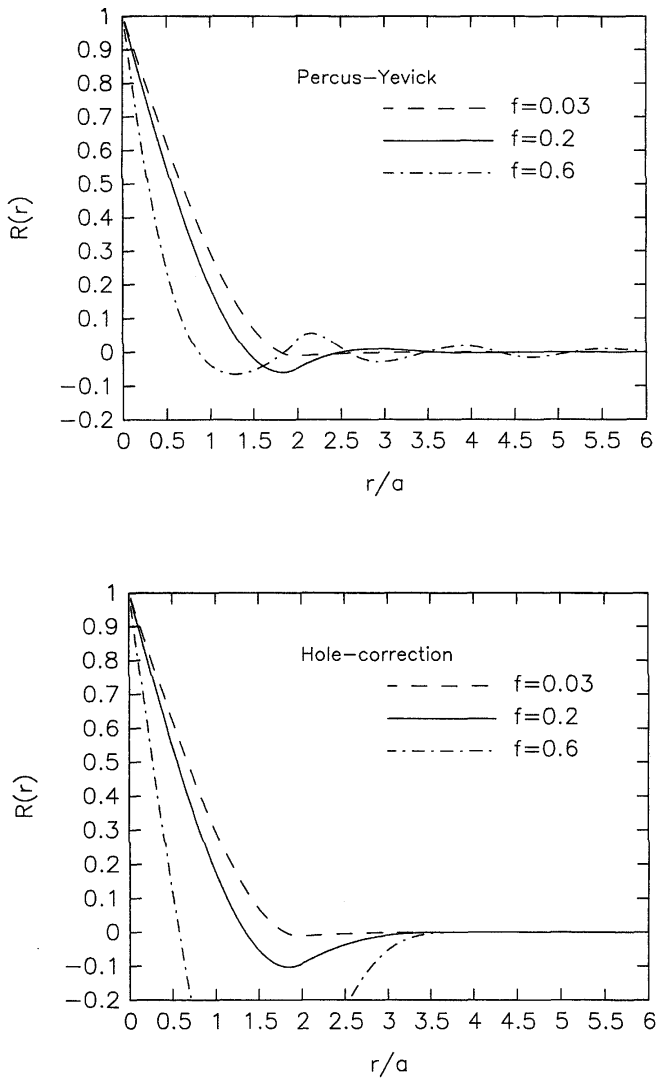


Figure 4. Comparisons of Percus-Yevick and Hole Correction results.

3.1.b Penetrable model

The correlation function for a random collection of penetrable spheres is obtained by first calculating $P_{11}(r)$, which is the probability of finding both ends of a rod of length r within medium 1 (background medium). This can be computed by considering a thought experiment of randomly adding spherical scatterers one by one into a total scattering volume V . Each addition of a scatterer is assumed to be independent of others. The probability of finding the two points outside the spheres is equivalent to that of having the sphere centers outside the union volume of two auxiliary spheres located with centers at each of the two endpoints (Figure 5).

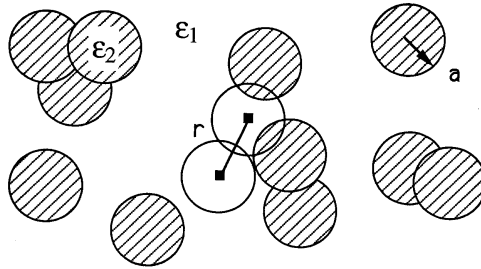


Figure 5. A collection of penetrable spheres.

Therefore, the probability function is given as

$$P_{11}(r) = \lim_{N \rightarrow \infty} \left[\frac{V - V_U(r)}{V} \right]^N = \lim_{N \rightarrow \infty} \left[1 - \frac{n_o V_U(r)}{N} \right]^N \tag{23}$$

where V_U is the union volume of spheres with centers located at the endpoints of the rod and N is the total number of scatterers. As the total number of scatterers approaches infinity, $P_{11}(r)$ approaches an exponential form.

$$P_{11}(r) = \exp[-n_o V_U(r)] \tag{24}$$

The union volume of two spheres of radius a which are separated by a distance r is given as

$$V_U(r) = \frac{4\pi a^3}{3} \left[1 + \frac{3r}{4a} - \frac{1}{16} \left(\frac{r}{a} \right)^3 \right] \quad r < 2a$$

$$= \frac{8\pi}{3}a^3 \quad r \geq 2a \quad (25)$$

Since the scatterers are allowed to interpenetrate each other, there is no direct proportional relation between the number density and the fractional volume unlike in the impenetrable case. To find this relation, we consider $P_{11}(0)$. $P_{11}(0)$ is the probability of finding a rod of length zero, or a point, within medium 1.

$$P_{11}(0) = \exp[-n_o V_{\cup}(0)] \quad (26)$$

This is simply one minus the fractional volume. The union volume at r equal to zero is just the volume of one sphere

$$1 - f = \exp[-n_o \frac{4}{3}\pi a^3] \quad (27)$$

Substituting these values in the original expression and solving for n_o , we arrive at the relation needed

$$n_o = -\frac{3}{4\pi a^3} \ln(1 - f) \quad (28)$$

On the other hand, the correlation function of the permittivity is given as

$$C(r) = |\epsilon_1 - \epsilon_2|^2 (\exp[-n_o V_{\cup}(r)] - (1 - f)^2) \quad (29)$$

which implies that the normalized correlation function can be written in the following form by substituting the expressions for the union volume and the number density into the definition of the correlation function:

$$\begin{aligned} R(r) &= \frac{1}{f}(1 - f)^{[3r/4a - (\frac{r}{a})^3/16]} - \frac{1}{f}(1 - f), \quad r < 2a \\ &= 0, \quad r \geq 2a \end{aligned} \quad (30)$$

Figure 6 shows the plot of normalized correlation functions for various fractional volumes. As in the impenetrable case, the function drops off faster as the fractional volume increases. However, there is no oscillation nor much variation as a function of fractional volume unlike in the impenetrable case.

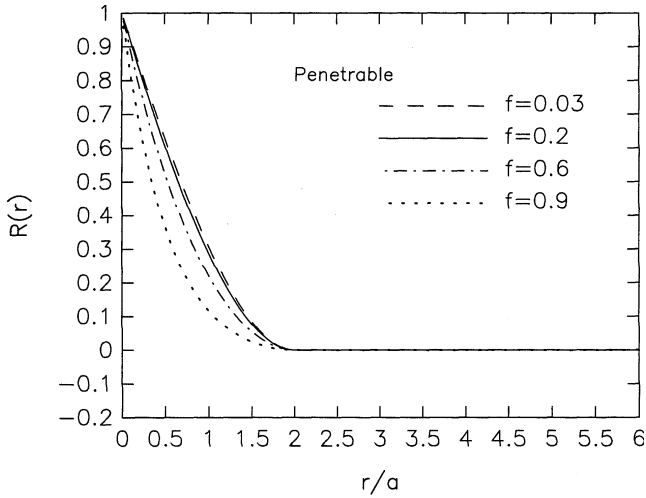


Figure 6. Normalized correlation functions for penetrable spheres.

3.2 Basic Formulation

In this section we discuss a novel technique to calculate the correlation function for a collection of impenetrable spheres with multiple sizes. As outlined in Section 1, the first step towards determining the correlation function is to solve the scattering problem using the random medium model employing the Born approximation. Assume permittivity fluctuations are weak so that $|\epsilon_2 - \epsilon_1| \ll \epsilon_1$. Let

$$\epsilon(\vec{r}) = \epsilon_1 + \epsilon_f(\vec{r}) \tag{31}$$

Here, ϵ_1 is the background permittivity which differs from the mean permittivity slightly and $\epsilon_f(\vec{r})$ represents the permittivity fluctuations. The wave equation for this configuration can be written as

$$\nabla \times \nabla \times \bar{E}(\vec{r}) - k^2 \bar{E}_o(\vec{r}) = \omega^2 \mu \epsilon_f(\vec{r}) \bar{E}(\vec{r}) = Q(\vec{r}) \bar{E}(\vec{r}) \tag{32}$$

where the right hand side acts as a random source. The solution can be written in terms of the dyadic Green's function $\bar{\bar{G}}(\vec{r}, \vec{r}')$ as

$$\bar{E}(\vec{r}) = \bar{E}^{(0)}(\vec{r}) + \int_{V_T} d\vec{r}' \bar{\bar{G}}(\vec{r}, \vec{r}') Q(\vec{r}') \bar{E}(\vec{r}') \tag{33}$$

where $\overline{E}^{(0)}$ is the solution in the absence of scatterers and V_T is the total volume that contains the scatterers. Under the Born approximation, the average scattered intensity takes the following form:

$$\begin{aligned} \langle |\overline{E}_s(\vec{r})|^2 \rangle &= \int_{V_T} \int_{V_T} d\vec{r}' d\vec{r}'' \overline{G}(\vec{r}, \vec{r}') \overline{E}^{(0)}(\vec{r}') \\ &\quad \left[\overline{G}(\vec{r}, \vec{r}'') \overline{E}^{(0)}(\vec{r}'') \right]^* \langle Q(\vec{r}') Q^*(\vec{r}'') \rangle \end{aligned} \quad (34)$$

In the far field the dyadic Green's function is

$$\overline{G}(\vec{r}, \vec{r}') = \frac{\epsilon^{ikr}}{4\pi r} [\hat{h}(\vec{k}_s) \hat{h}(\vec{k}_s) + \hat{v}(\vec{k}_s) \hat{v}(\vec{k}_s)] \epsilon^{-i\vec{k}_s \cdot \vec{r}'} \quad (35)$$

and if the homogeneous solution is taken as

$$\overline{E}^{(0)} = E_o \hat{h}(\vec{k}_i) \epsilon^{i\vec{k}_i \cdot \vec{r}} \quad (36)$$

the scattered intensity becomes

$$\langle |\overline{E}_s(\vec{r})|^2 \rangle = \frac{|E_o|^2}{16\pi^2 r^2} k^4 [|\hat{h}(\vec{k}_s) \hat{h}(\vec{k}_s) + \hat{v}(\vec{k}_s) \hat{v}(\vec{k}_s)] \cdot \hat{h}(\vec{k}_i)|^2 B(\vec{k}_i - \vec{k}_s) \quad (37)$$

with

$$\begin{aligned} B(\vec{k}_i - \vec{k}_s) &= \int_{V_T} \int_{V_T} d\vec{r}' d\vec{r}'' \langle \epsilon_{rf}(\vec{r}') \epsilon_{rf}^*(\vec{r}'') \rangle \epsilon^{i(\vec{k}_i - \vec{k}_s) \cdot (\vec{r}' - \vec{r}'')} \\ &= \epsilon_{rf}^2 \int_{V_T} \int_{V_T} d\vec{r}' d\vec{r}'' \langle H(\vec{r}') H(\vec{r}'') \rangle \epsilon^{i(\vec{k}_i - \vec{k}_s) \cdot (\vec{r}' - \vec{r}'')} \\ &= \epsilon_{rf}^2 \int_{V_T} \int_{V_T} d\vec{r}' d\vec{r}'' P_{22}(\vec{r}' - \vec{r}'') \epsilon^{i(\vec{k}_i - \vec{k}_s) \cdot (\vec{r}' - \vec{r}'')} \end{aligned} \quad (38)$$

where Equation (16) has been used and ϵ_{rf} is assumed to be real.

When V_T is large compared to the spread of P_{22} , $B(\vec{k}_i - \vec{k}_s)$ can be approximated as

$$B(\vec{k}_i - \vec{k}_s) \simeq \epsilon_{rf}^2 V_T \int_{-\infty}^{\infty} d\vec{r}' P_{22}(\vec{r}') \epsilon^{i(\vec{k}_i - \vec{k}_s) \cdot \vec{r}'} \quad (39)$$

giving a Fourier relation. It is this relation which makes it possible to solve for the correlation function when the scattering problem is solved with another model and the two results are equated.

For the configuration considered, $P_{22}(\bar{r})$ is isotropic so that $P_{22}(\bar{r}) = P_{22}(r)$ and

$$B(h) = \epsilon_{rf}^2 V_T \int_0^\infty dr P_{22}(r) \frac{4\pi r}{h} \sin hr \tag{40}$$

where

$$h = |\bar{k}_i - \bar{k}_s| \tag{41}$$

Therefore, in terms of $B(h)$ the probability function can be evaluated as

$$r P_{22}(r) = \frac{1}{\epsilon_{rf}^2 V_T 2\pi^2} \int_0^\infty dh B(h) h \sin hr \tag{42}$$

For the next step, we calculate $B(h)$ using the discrete scatterer model. The problem will be solved for sparse and dense distribution of particles separately.

3.3 Sparse Distribution of Particles

Consider a single sphere of radius a located at the origin. Under Born approximation, the scattered field can be written as

$$\bar{E}_s = \frac{\epsilon^{ikr}}{4\pi r} E_o k^2 [\hat{h}(\bar{k}_s) \hat{h}(\bar{k}_s) + \hat{v}(\bar{k}_s) \hat{v}(\bar{k}_s)] \cdot \hat{h}(\bar{k}_i) \epsilon_{rf} V_a F(|\bar{k}_i - \bar{k}_s|a) \tag{43}$$

Where V_a is the volume of the sphere and $F(ha)$ determines the scattering pattern and is given as

$$F(ha) = \frac{3}{h^3 a^3} (\sin ha - ha \cos ha) \tag{44}$$

Assuming incoherent addition of power, the scattering intensity for the discrete scatterer model becomes

$$\begin{aligned} \langle |\bar{E}_s(\bar{r})|^2 \rangle &= \frac{|E_o|^2}{16\pi^2 r^2} k^4 |[\hat{h}(\bar{k}_s) \hat{h}(\bar{k}_s) + \hat{v}(\bar{k}_s) \hat{v}(\bar{k}_s)] \cdot \hat{h}(\bar{k}_i)|^2 \\ &\quad \cdot \epsilon_{rf}^2 N_T \int_0^\infty da p(a) F^2(ha) V_a^2 \end{aligned} \tag{45}$$

where N_T is the total number of scatterers and $p(a)$ is the size density function. Comparing Equations (37) and (45) we see that

$$B(h) = \epsilon_{rf}^2 N_T \int_0^\infty da p(a) F^2(ha) V_a^2 \quad (46)$$

so that using Equation (42) the probability function can be obtained as

$$P_{22}(r) = 8 \frac{N_T}{V_T} \int_0^\infty dh h^2 \frac{\sin hr}{hr} \int_0^\infty da' p(a') \left(\frac{\sin ha' - ha' \cos ha'}{h^3} \right)^2 \quad (47)$$

which relates the size distribution function to the probability function for impenetrable particles. It should be noted that this equality is exact in the limit as the fractional volume goes to zero since we assumed incoherent addition of power in the discrete scatterer model. If we assume all the particles have identical size so that $p(a') = \delta(a' - a)$, the probability function becomes

$$P_{22}(r) = 8 \frac{N_T}{V_T} \frac{a^6}{r} \int_0^\infty dh h \sin hr \left(\frac{\sin ha - ha \cos ha}{h^3 a^3} \right)^2 \quad (48)$$

$$= f \left[1 - \frac{3}{4} \left(\frac{r}{a} \right) + \frac{1}{16} \left(\frac{r}{a} \right)^3 \right] \quad 0 \leq r \leq 2a \quad (49)$$

where f denotes the fractional volume of the scatterers. The second equality is obtained using the identity

$$\frac{6}{\pi} \int_0^\infty du u^2 \left(\frac{\sin u - u \cos u}{u^3} \right)^2 \frac{\sin u \alpha}{u \alpha} = 1 - \frac{3}{4} \alpha + \frac{1}{16} \alpha^3 \quad 0 \leq \alpha \leq 2 \quad (50)$$

Note that the common volume between two spheres of radius a whose centers are separated by r is given as

$$V \cap (r, a) = \begin{cases} \frac{4\pi}{3} a^3 \left[1 - \frac{3}{4} \left(\frac{r}{a} \right) + \frac{1}{16} \left(\frac{r}{a} \right)^3 \right], & 0 \leq r \leq 2a \\ 0, & \text{otherwise} \end{cases}$$

which indicates that the expression given in Equation (49) is determined by this function. This result is true for sparse distribution of

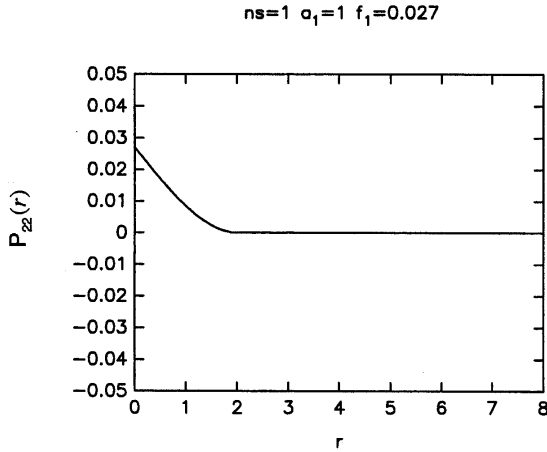
particles and additional terms are required for the general case as indicated by Equation (21). Note that in the sparse distribution result, f^2 term is neglected. The derivation of the general result will be given when we treat densely distributed particles. Using Equation (47) the probability function can also be expressed as

$$\begin{aligned}
 P_{22}(r) &= 8 \frac{N_T}{V_T} \int_0^\infty da p(a) a^6 \int_0^\infty dh h^2 \frac{\sin hr}{hr} \left(\frac{\sin ha - ha \cos ha}{h^3 a^3} \right)^2 \quad (52) \\
 &= \frac{N_T}{V_T} \int_0^\infty da V_\cap(r, a) p(a) \quad (53)
 \end{aligned}$$

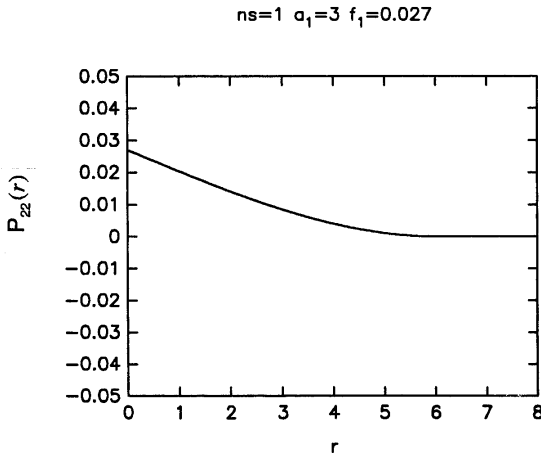
where $V_\cap(r, a)$ is given in Equation (51). This is the final expression for the probability function of sparsely distributed spheres with the size distribution described by $p(a)$. Given this expression, the correlation function can be determined easily using Equation (17).

In Figure 7 the effect of particle size on the correlation function is demonstrated. It is seen that the correlation length (the length at which the correlation function decreases to 37% of its peak value) increases with increasing particle size. This is expected since for sparse distribution of particles, the correlation function is determined by the common volume between two spheres of radius a which are displaced with respect to each other by a distance of r (see Equations (17), (49), and (51)). For sparse distribution of particles the correlation function can be computed for any size distribution using Equations (53) and (17). In Figure 8 we demonstrate the effect of multiple scales on the correlation function. Here two species are considered with different particle sizes and fractional volumes. In these figures ns is the number of species, f_1 and f_2 denote fractional volumes for the respective species and a_1 and a_2 represent corresponding radii. Note that in Figure 8a the parameters are chosen such that species contribute equally to the scattered field under the Rayleigh scattering approximation. This condition requires $f_1 a_1^3 = f_2 a_2^3$ since the scattered power from a given particle is proportional to the sixth power of the radius. The comparison between Figures 7a and 8a is very significant because we see that the functions are only slightly different from each other although the scattered power is twice as high in the latter case. This indicates the importance of considering multiple size in the computation or measurement of correlation functions. In Figure 8b the effect of multiple sizes

is seen more clearly as giving the probability function a characteristic shape with two scales. In other words, it is not possible to describe such a medium with a single correlation length since the scattering properties of that medium would be significantly different.



(a)



(b)

Figure 7. Effect of particle size on correlation length.

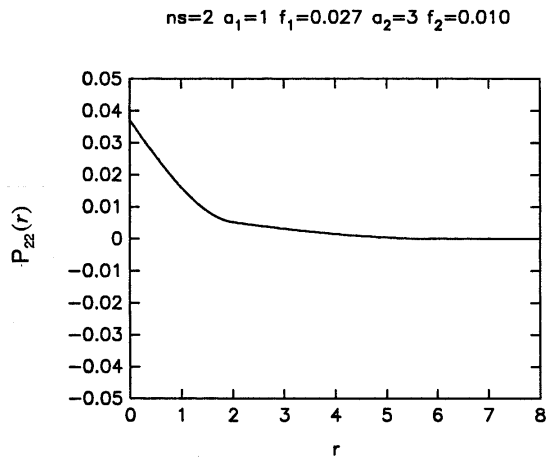
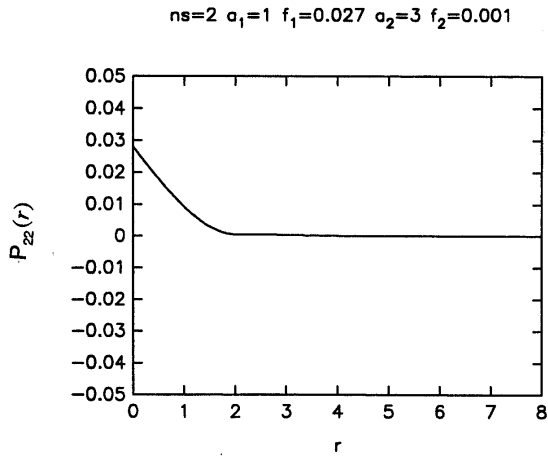


Figure 8. Effect of multiple scales on correlation function.

The fact that the correlation function is related to the common volume of two intersecting particles is not peculiar to spherical particles only. In fact, in the following we show that this is the case for particles of arbitrary shape. For this purpose, consider the scattered field from a particle of arbitrary shape. Under Born approximation,

$$\bar{E}_s = \frac{\epsilon^{ikr}}{4\pi r} E_o k^2 [\hat{h}(\bar{k}_s) \hat{h}(\bar{k}_s) + \hat{v}(\bar{k}_s) \hat{v}(\bar{k}_s)] \cdot \hat{h}(\bar{k}_i) \epsilon_{rf} \int_V d\bar{r}' \epsilon^{i(\bar{k}_i - \bar{k}_s) \cdot \bar{r}'} \quad (54)$$

where V denotes the volume of the scatterer. Therefore, the scattered intensity is

$$\begin{aligned} \langle |\bar{E}_s(\bar{r})|^2 \rangle &= \frac{|E_o|^2}{16\pi^2 r^2} k^4 [|\hat{h}(\bar{k}_s) \hat{h}(\bar{k}_s) + \hat{v}(\bar{k}_s) \hat{v}(\bar{k}_s)] \\ &\quad \cdot |\hat{h}(\bar{k}_i)|^2 \epsilon_{rf}^2 \cdot \int_V \int_V d\bar{r}' d\bar{r}'' \epsilon^{i(\bar{k}_i - \bar{k}_s) \cdot (\bar{r}' - \bar{r}'')} \quad (55) \end{aligned}$$

Using Equations (37) and (39), we see that

$$\epsilon_{rf}^2 N_T \int_V \int_V d\bar{r}' d\bar{r}'' \epsilon^{i(\bar{k}_i - \bar{k}_s) \cdot (\bar{r}' - \bar{r}'')} = \epsilon_{rf}^2 V_T \int_{-\infty}^{\infty} d\bar{r}' P_{22}(\bar{r}') \epsilon^{i(\bar{k}_i - \bar{k}_s) \cdot \bar{r}'} \quad (56)$$

Introducing $U(\bar{r})$ which is unity on a given particle and zero elsewhere (note the difference between $U(\bar{r})$ and $H(\bar{r})$, where the latter is unity on all particles) we obtain

$$\begin{aligned} &\int_V \int_V d\bar{r}' d\bar{r}'' \epsilon^{i(\bar{k}_i - \bar{k}_s) \cdot (\bar{r}' - \bar{r}'')} \\ &= \int_{-\infty}^{\infty} d\bar{r}' U(\bar{r}') \int_{-\infty}^{\infty} d\bar{r}'' U(\bar{r}'') \epsilon^{i(\bar{k}_i - \bar{k}_s) \cdot (\bar{r}' - \bar{r}'')} \\ &= \int_{-\infty}^{\infty} d\bar{r}' U(\bar{r}') \int_{-\infty}^{\infty} d\bar{r}'' U(\bar{r}' - \bar{r}'') \epsilon^{i(\bar{k}_i - \bar{k}_s) \cdot \bar{r}''} \\ &= \int_{-\infty}^{\infty} d\bar{r}'' \epsilon^{i(\bar{k}_i - \bar{k}_s) \cdot \bar{r}''} \int_{-\infty}^{\infty} d\bar{r}' U(\bar{r}') U(\bar{r}' - \bar{r}'') \quad (57) \end{aligned}$$

so that

$$P_{22}(\bar{r}) = \frac{N_T}{V_T} \int_{-\infty}^{\infty} d\bar{r}' U(\bar{r}') U(\bar{r}' - \bar{r}) \quad (58)$$

It is seen that the integral gives the common volume between intersecting particles separated by \bar{r} .

3.3.a Correlation function vs. size distribution

The relationship between the correlation function and the size distribution function was established above. Equations (17) and (53) demonstrate that when the size distribution of a collection of sparsely distributed particles is known the correlation function can be computed. In this section we will discuss the inverse problem of calculating the size distribution function when the correlation function is known. Mathematically this requires the solution of the integral equation given as

$$P_{22}(r) = \frac{N_T}{V_T} \int_0^\infty da p(a) \frac{4\pi}{3} a^3 \left[1 - \frac{3}{4} \left(\frac{r}{a}\right) + \frac{1}{16} \left(\frac{r}{a}\right)^3 \right] \quad (59)$$

In this equation we wish to determine $p(a)$ when $P_{22}(r)$ is known for all r .

An integral equation of the form (59) can be solved using the Mellin transform. The integral

$$\Phi(z) = \int_0^\infty dx x^{z-1} \phi(x) \quad (60)$$

is called the Mellin transform of the function $\phi(x)$ with respect to the complex parameter z . If $\Phi(z)$ is regular in the strip $S = \{z : a < \sigma < b\}$, then the inverse transformation is given as

$$\phi(x) = \frac{1}{2\pi i} \int_{c-i\infty}^{c+i\infty} dz x^{-z} \Phi(z) \quad (61)$$

where $a < c < b$. An important property of the Mellin transform is the relation

$$\int_0^\infty dt \phi_1(x/t) \phi_2(t) \rightarrow \Phi_1(z) \Phi_2(z+1) \quad (62)$$

which implies that an integral equation of the form

$$g(y) = \int_0^\infty dx f(x) k(y/x) \quad (63)$$

can be solved for $f(x)$ as

$$f(x) = \frac{1}{2\pi i} \int_{c-i\infty}^{c+i\infty} dz x^{-z} \frac{G(z-1)}{K(z-1)} \quad (64)$$

where $G(z)$ and $K(z)$ are the Mellin transforms of $g(y)$ and $k(y)$, respectively.

Employing these properties, Equation (59) can be solved to obtain an explicit expression for the size distribution function in terms of the correlation function as

$$p(a) = \frac{a^{-3}}{2\pi i} \int_{c-i\infty}^{c+i\infty} dz a^{-z} \frac{(z-1)z(z+2)}{2^{z-2}6} \int_0^\infty dr P'_{22}(r) r^{z-2} \quad (65)$$

where $P'_{22}(r) = 3V_T/(4\pi N_T)P_{22}(r)$. This equation indicates that there is a one-to-one relationship between the size distribution function and the correlation function for sparsely distributed particles and that this relationship can be expressed in terms of explicit formulas given by (59) and (65).

3.3.b Thin sections and correlation functions

Thin sections are commonly used in sea ice research to determine the correlation function of a random medium [26,27]. A thin section is obtained by cutting a block of ice into a thin layer and marking the scatterers. The correlation function is then calculated by correlating the thin section with its replica which is displaced from the original by a distance r . In the following we will show that this process does in fact provide the correct correlation function as defined above. This is not obvious because in the process, a two-dimensional cut of the three-dimensional random medium is used.

Consider a collection of spheres with unity radius which are uniformly distributed in a given volume V . When a cut is made through the volume, the cutting plane will intercept some of the spheres and the centers of the intercepted spheres will be at different distances from the cutting plane. Therefore, the intersection of the spheres and the cutting plane will consist of circles with varying radii. Since the number density is uniformly distributed as a function of distance from the cutting plane, the number distribution as a function of circle radius takes the form

$$n(a) = \frac{2n_o a}{\sqrt{1-a^2}} \quad (66)$$

where n_o is the volume number density, and a is the radius of circles on the cutting plane (Figure 9).

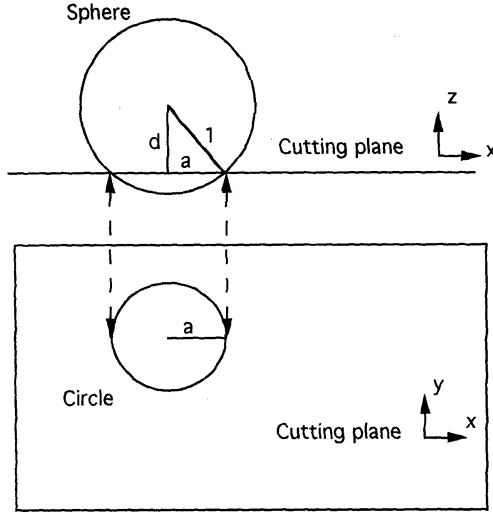


Figure 9. Intersection of the cutting plane and a sphere.

When the thin sections are displaced by a distance r and the common area between displaced circles are calculated, the following integral is obtained which gives the probability function:

$$P_{22}(r) = \int_{r/2}^1 da \frac{2n_o a}{\sqrt{1-a^2}} 2 \left(a^2 \cos^{-1} \frac{r}{2a} - \frac{r}{2} \sqrt{a^2 - \frac{r^2}{4}} \right) \quad (67)$$

where we have used the fact that the common area between two circles of radius a which are displaced by a distance of r is given as

$$A_{\cap} = 2 \left(a^2 \cos^{-1} \frac{r}{2a} - \frac{r}{2} \sqrt{a^2 - \frac{r^2}{4}} \right) \quad (68)$$

Upon evaluating the integral of (67) we obtain

$$P_{22}(r) = \frac{4\pi}{3} n_o \left(1 - \frac{3}{4}r + \frac{1}{16}r^3 \right) \quad r < 2a \quad (69)$$

as before.

Although we have shown that the thin section analysis provides the correct correlation function for a collection of sparsely distributed spheres with identical radii, this result is far more general. In fact for any isotropic random medium, each thin section should give the same result due to symmetry, but the volume calculation can be obtained from a stack of thin sections each of which gives identical result; therefore thin section result (2-D) must be identical to volume result (3-D) for any isotropic random medium. However, this is true only in the limit when the thickness of thin sections goes to zero. In practice the ability to obtain volume information from thin sections is limited by the actual thickness of thin sections compared to the size of the smaller particles.

3.4 Dense Distribution of Particles

When particles are densely distributed, pair distribution functions are needed to describe the structure of the medium. To calculate scattered fields, consider a collection of spherical particles which have identical size. Let the center of the i th particle be at \bar{r}_i (Figure 10). Under the Born approximation the scattered field from this particle can be written as

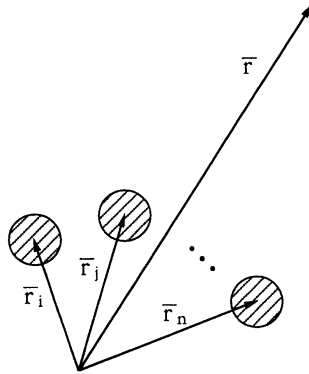


Figure 10. Configuration for densely distributed particles.

$$\begin{aligned} \bar{E}_s = & \frac{\epsilon^{ikr}}{4\pi r} E_o k^2 [\hat{h}(\bar{k}_s) \hat{h}(\bar{k}_s) + \hat{v}(\bar{k}_s) \hat{v}(\bar{k}_s)] \\ & \cdot \hat{h}(\bar{k}_i) \epsilon_{rf} \int_V d\bar{r}' \epsilon^{i(\bar{k}_i - \bar{k}_s) \cdot \bar{r}'} \epsilon^{i(\bar{k}_i - \bar{k}_s) \cdot \bar{r}_i} \end{aligned} \quad (70)$$

which implies that the total scattered field is

$$\bar{E}_s = \sum_{i=1}^{N_T} \bar{A} J_i \tag{71}$$

where $J_i = \exp(i(\bar{k}_i - \bar{k}_s) \cdot \bar{r}_i)$ is the phase factor and \bar{A} is the scattered field from a particle located at the origin.

Similarly, the scattered intensity can be expressed as

$$|\bar{E}_s(\bar{r})|^2 = |\bar{A}|^2 [N_T + \sum_{i=1}^{N_T} \sum_{j>i} 2\text{Re}\{J_i J_j^*\}] \tag{72}$$

Upon ensemble averaging, we obtain

$$\langle |\bar{E}_s(\bar{r})|^2 \rangle = |\bar{A}|^2 [N_T + L] \tag{73}$$

where

$$L = \sum_{i=1}^{N_T} \sum_{j>i} 2\text{Re} \int d\bar{r}_1 \dots d\bar{r}_{N_T} p(\bar{r}_1 \dots \bar{r}_{N_T}) \epsilon^{i(\bar{k}_i - \bar{k}_s) \cdot (\bar{r}_i - \bar{r}_j)} \tag{74}$$

Here $p(\bar{r}_1 \dots \bar{r}_{N_T})$ denotes N -point distribution function. Note that incoherent addition assumption is not made. Performing $(N_T - 2)$ -fold integration and summing we obtain

$$L = N_T(N_T - 1) \text{Re} \int_{V_T} \int_{V_T} d\bar{r}_i d\bar{r}_j p_2(\bar{r}_i, \bar{r}_j) \epsilon^{i(\bar{k}_i - \bar{k}_s) \cdot (\bar{r}_i - \bar{r}_j)} \tag{75}$$

$$\simeq \frac{N_T^2}{V_T^2} \text{Re} \int_{V_T} \int_{V_T} d\bar{r}_i d\bar{r}_j g(\bar{r}_i, \bar{r}_j) \epsilon^{i(\bar{k}_i - \bar{k}_s) \cdot (\bar{r}_i - \bar{r}_j)} \tag{76}$$

where $g(\bar{r}_i, \bar{r}_j)$ is commonly known as the pair distribution function. Using this equation, the averaged scattered intensity can be written as

$$\begin{aligned} \langle |\bar{E}_s(\bar{r})|^2 \rangle &= \frac{|E_o|^2}{16\pi^2 r^2} k^4 |[\hat{h}_s \hat{h}_s + \hat{v}_s \hat{v}_s] \cdot \hat{h}_i|^2 \\ &\quad \{ \epsilon_{rf}^2 N_T \int_{V_s} \int_{V_s} d\bar{r}' d\bar{r}'' \epsilon^{i(\bar{k}_i - \bar{k}_s) \cdot (\bar{r}' - \bar{r}'')} \} \end{aligned}$$

$$\begin{aligned}
 & + \epsilon_{rf}^2 \int_{V_s} \int_{V_s} d\bar{r}' d\bar{r}'' \epsilon^{i(\bar{k}_i - \bar{k}_s) \cdot (\bar{r}' - \bar{r}'')} \\
 n_o^2 Re \int_{V_T} \int_{V_T} d\bar{r}_i d\bar{r}_j g(\bar{r}_i, \bar{r}_j) & \epsilon^{i(\bar{k}_i - \bar{k}_s) \cdot (\bar{r}_i - \bar{r}_j)} \} \quad (77)
 \end{aligned}$$

where V_s denotes the volume of the sphere and n_o is the number density. An equation for the probability function can be obtained by comparing Equations (37) and (77). Defining the function $U(\bar{r})$ as before we get

$$\begin{aligned}
 & \int_{V_T} \int_{V_T} d\bar{r}' d\bar{r}'' P_{22}(\bar{r}' - \bar{r}'') \epsilon^{i\bar{\alpha} \cdot (\bar{r}' - \bar{r}'')} \\
 & = N_T \int_{V_T} \int_{V_T} d\bar{r}' d\bar{r}'' U(\bar{r}') U(\bar{r}'') \epsilon^{i\bar{\alpha} \cdot (\bar{r}' - \bar{r}'')} \\
 & + n_o^2 \int_{V_T} \int_{V_T} d\bar{r}' d\bar{r}'' U(\bar{r}') U(\bar{r}'') \epsilon^{i\bar{\alpha} \cdot (\bar{r}' - \bar{r}'')} \\
 & \cdot Re \int_{V_T} \int_{V_T} d\bar{r}_i d\bar{r}_j g(\bar{r}_i, \bar{r}_j) \epsilon^{i\bar{\alpha} \cdot (\bar{r}_i - \bar{r}_j)} \quad (78)
 \end{aligned}$$

where $\bar{\alpha} = \bar{k}_i - \bar{k}_s$. After some manipulations, the solution of this equation for the probability function gives

$$P_{22}(\bar{r}) = f C_o(\bar{r}) + f^2 \int_{-\infty}^{\infty} d\bar{r}' g(\bar{r}') \frac{C_o(\bar{r}' - \bar{r})}{V_s} \quad (79)$$

where f is the fractional volume of the scatterers and

$$C_o(\bar{r}) = \frac{1}{V_s} \int_{-\infty}^{\infty} d\bar{r}' U(\bar{r}') U(\bar{r}' - \bar{r}) \quad (80)$$

Note that the first term is identical to the result we got for sparsely distributed particles, which indicates that for sparsely distributed particles the second order term in fractional volume is neglected. It can also be shown that this result is identical to that of Equation (21).

In Figure 11 we show that numerical results for a collection of densely distributed particles where it is assumed that $|\epsilon_1 - \epsilon_2| = 1$. The pair distribution function for the configuration is shown in Figure 11a. This function is evaluated using the algorithm described below.

In Figure 11b the “intrinsic” correlation function (self-term) is demonstrated. This function does not include the interaction term between different particles and is given by the common volume between two spheres displaced with respect to each other. The interaction term which involves the pair distribution function is depicted in Figure 11c. The actual correlation function which includes both the intrinsic correlation function and the interaction term is depicted in 11d. It is seen that for densely distributed particles interaction term is significant and the correlation function might become negative.

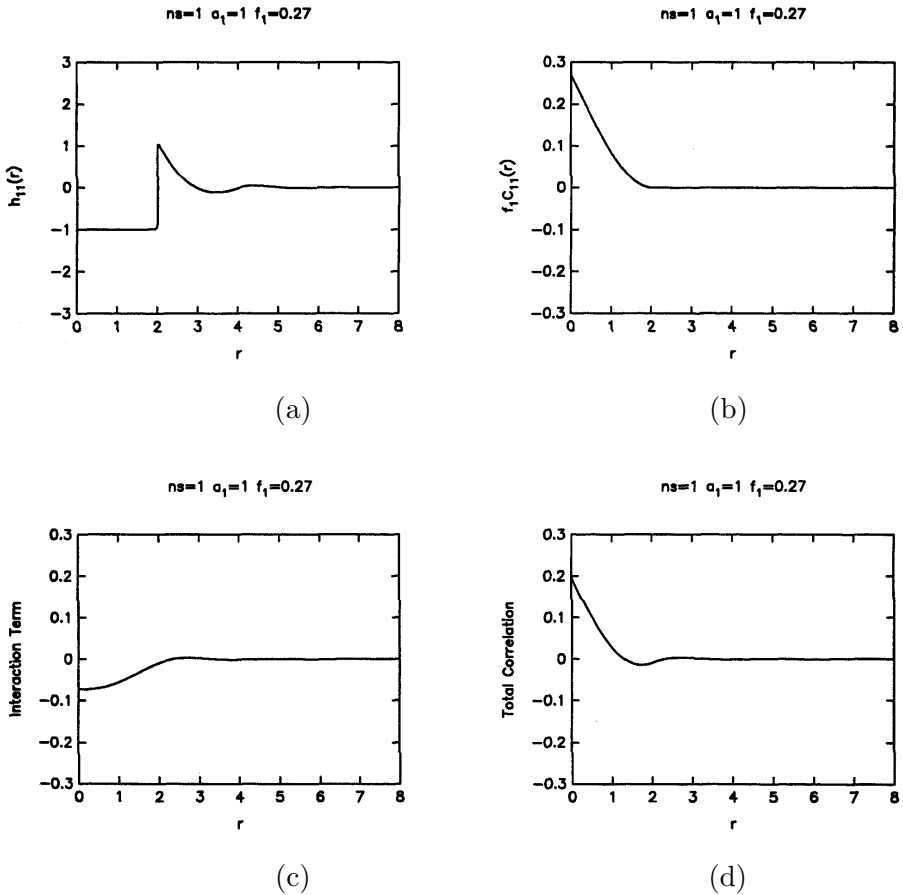


Figure 11. Single scale densely distributed particles.

For a two-component system which consists of particles of two different sizes, the method can be easily extended. For this case, two-component pair distribution functions are introduced. The final result can be obtained as

$$\begin{aligned}
 P_{22}(\bar{r}) &= f_1 C_{11}(\bar{r}) + f_1^2 \int_{-\infty}^{\infty} d\bar{r}' g_{11}(\bar{r}') \frac{C'_{11}(\bar{r}' - \bar{r})}{V_1 V_1} \\
 &+ f_2 C_{22}(\bar{r}) + f_2^2 \int_{-\infty}^{\infty} d\bar{r}' g_{22}(\bar{r}') \frac{C'_{22}(\bar{r}' - \bar{r})}{V_2 V_2} \\
 &+ 2f_1 f_2 \int_{-\infty}^{\infty} d\bar{r}' g_{12}(\bar{r}') \frac{C'_{12}(\bar{r}' - \bar{r})}{V_1 V_2}
 \end{aligned} \tag{81}$$

where f_i and V_i denote fractional volumes and particle volumes for the two components ($i = 1, 2$), respectively. Pair distribution functions are expressed as g_{ij} , and

$$C'_{ij}(\bar{r}) = \int_{-\infty}^{\infty} d\bar{r}' U_i(\bar{r}') U_j(\bar{r}' - \bar{r}) \tag{82}$$

It is easy to see that

$$\lim_{\bar{r} \rightarrow 0} P_{22}(\bar{r}) = f_1 + f_2 \tag{83}$$

and

$$\lim_{\bar{r} \rightarrow \infty} P_{22}(\bar{r}) = (f_1 + f_2)^2 \tag{84}$$

as expected.

Figures 12 and 13 demonstrate results for a two scale densely distributed collection of particles. In 12 pair distribution functions are depicted and in 13, the corresponding correlation functions are illustrated ($|\epsilon_1 - \epsilon_2| = 1$). The effect of the interaction term is again clearly seen which indicates that as the density of the particles increases the scale of correlation decreases.

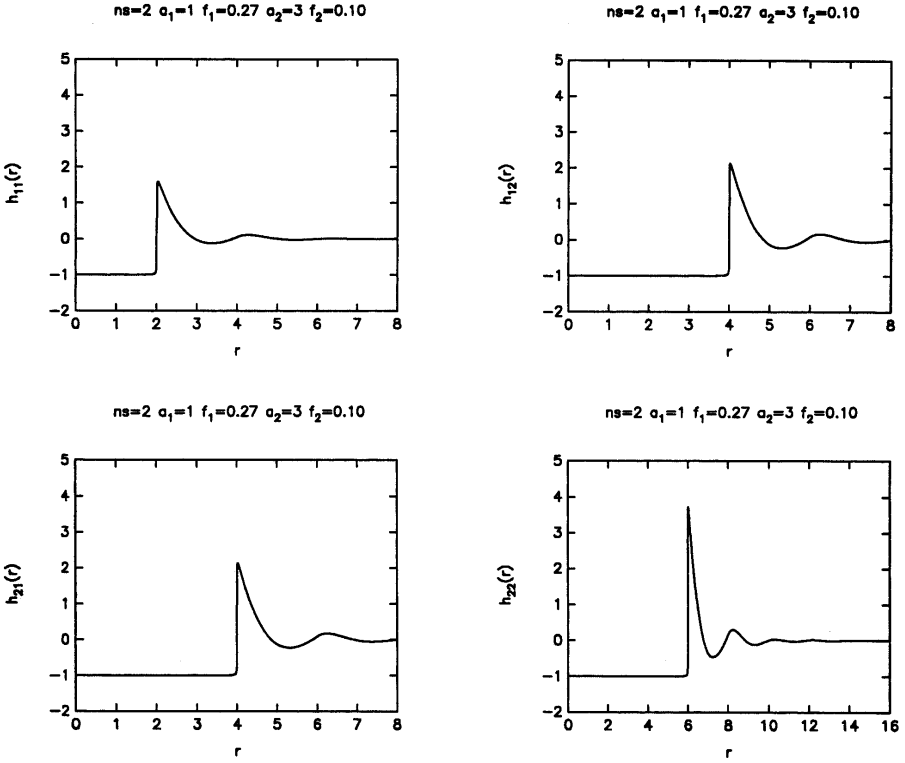


Figure 12. Pair distribution functions for two scale densely distributed particles.

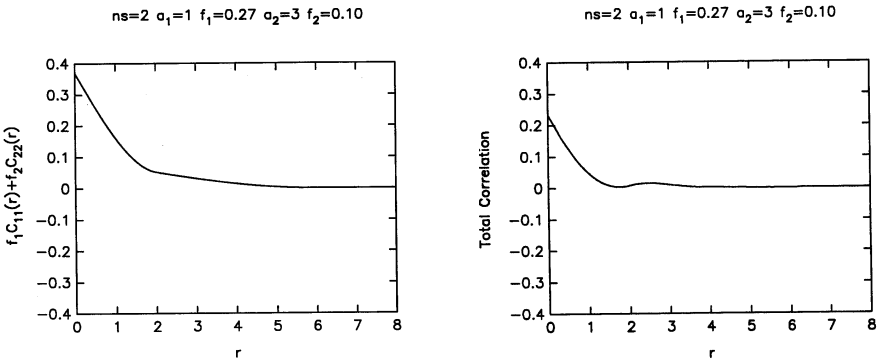


Figure 13. Correlation functions for two scale densely distributed particles.

4. Summary and Conclusions

In this chapter, a continuous random medium model was considered to describe a collection of multi-scale spherical scatterers to determine the correlation function for this configuration. Sparse and dense distribution of particles were considered separately. For sparse distribution of particles it was shown that the correlation function can be expressed in terms of the common volume between two spheres displaced with respect to each other. For densely distributed particles pair distribution functions were introduced and the correlation functions were related to them. Various physical configurations were investigated by changing the size and fractional volume of the particles.

To determine the correlation function, a novel technique was used: The scattering problem was first solved by the continuous random medium model leaving the correlation function as unknown. The scattering problem was then solved by the discrete scatterer model which requires the specification of shapes and distributions of the scatterers but not the correlation function. Finally, the results from two approaches were equated to obtain an equation for the correlation function. The solution of this equation was facilitated by treating the weak scattering case and employing the Born approximation. However, the result has been shown to be valid in general since the correlation function is a function of the geometric organization of the particles and independent of their scattering properties.

In this study, the emphasis has been on the consideration of multiple size spheres. It is very important to consider multiple sizes since in the Rayleigh limit scattering cross section of spherical particles is proportional to the sixth power of the radius. This nonlinear relation results in significant scattering from larger particles even if their number density is small. An accurate correlation function should reflect this effect. In fact it has been observed that multiple sizes give the correlation function a characteristic shape which can be subtle although resultant scattering is significant. This is the counterpart of the discrete scatterer picture in which a small number of larger particles can contribute as much as a great number of smaller particles. Since different size particles are reflected in the correlation function with the presence of different scales it is in general not possible to describe the configuration accurately with a single correlation length.

It has also been shown that there is a one-to-one correspondence between the size distribution function and the correlation function for sparsely distributed particles and that this relationship can be expressed in terms of explicit formulas, which means that given the correlation function, the size distribution function can be calculated and vice versa.

5. Appendix

Multi-Component Pair Distribution Functions

In Equation (81) the correlation function is related to the multi-component pair distribution functions. In the following we give a review of the Percus-Yevick approximation and the computation of the pair distribution functions [28–29].

The pair distribution function $g_{ij}(r)$ is proportional to the conditional probability of finding a particle of type j at a distance r from the origin given that there is a particle of type i at the origin. A related function $h_{ij}(r)$ is defined as

$$h_{ij}(r) = g_{ij}(r) - 1 \quad (85)$$

The generalized Ornstein-Zernike relation [30]-[31], relates $h_{ij}(r)$ to $c_{ij}(r)$, the direct function, as

$$h_{ij}(r) = c_{ij}(r) + \sum_{l=1}^L n_l \int d\bar{r}' c_{il}(r') h_{lj}(|\bar{r} - \bar{r}'|) \quad (86)$$

where L is the number of species, and n_l are corresponding number densities.

Under Percus-Yevick approximation, the interparticle forces are zero except for the fact that two particles cannot interpenetrate each other. Let a_i and a_j be the particle radii of species i and j respectively. Then

$$g_{ij}(r) = 0, \quad r < a_i + a_j \quad (87)$$

Similarly, it is assumed that for non-interpenetrable particles $c_{ij}(r)$ is zero for separations larger than $a_i + a_j$. Thus,

$$c_{ij}(r) = 0, \quad r > a_i + a_j \quad (88)$$

Next, let

$$Y_{ij}(r) = \begin{cases} -c_{ij}(r), & r \leq R_{ij} \\ g_{ij}(r), & r > R_{ij} \end{cases} \quad (89)$$

where $R_{ij} = a_i + a_j$. Then using (85),(87)-(89), the Ornstein-Zernike relation can be expressed entirely in terms of Y_{ij} .

$$\begin{aligned} Y_{ij}(r) = 1 + & \sum_{l=1}^L n_l \int_{r' < R_{lj}; |\bar{r} - \bar{r}'| < R_{li}} d\bar{r}' Y_{il}(r') \\ & - \sum_{l=1}^L n_l \int_{r' < R_{lj}; |\bar{r} - \bar{r}'| < R_{li}} d\bar{r}' [Y_{il}(\bar{r} - \bar{r}') - 1] Y_{lj}(r') \\ & i, j = 1, 2, \dots, L \end{aligned} \quad (90)$$

The Equation (90) for the case of single species has been solved by Wertheim [31]. The solution for the case of two species can be found in Lebowitz [30]. For the general case of L species, the solution is obtained by Baxter [28] based on a generalized Wiener-Hopf technique:

Let $\tilde{H}_{ij}(\bar{p})$ and $\tilde{C}_{ij}(\bar{p})$ be proportional to the three dimensional Fourier transform of $h_{ij}(\bar{r})$ and $c_{ij}(\bar{r})$ as follows

$$\tilde{H}_{ij}(\bar{p}) = (n_i n_j)^{1/2} \int d\bar{r} e^{i\bar{p} \cdot \bar{r}} h_{ij}(\bar{r}) \quad (91)$$

$$\tilde{C}_{ij}(\bar{p}) = (n_i n_j)^{1/2} \int d\bar{r} e^{i\bar{p} \cdot \bar{r}} c_{ij}(\bar{r}) \quad (92)$$

then in matrix form the Ornstein-Zernike relation becomes

$$\tilde{H}(p) = \tilde{C}(p) + \tilde{C}(p)\tilde{H}(p) \quad (93)$$

Because of spherical symmetry, the transform only depends on $p = |\bar{p}|$. The matrices are of size $L \times L$. Using the generalized Wiener-Hopf technique, the solution of (93) can be factorized as [28]

$$\tilde{C}(p) = E - \tilde{Q}^T(-p)\tilde{Q}(p) \quad (94)$$

where E is the $L \times L$ unit matrix, and the subscript T denotes transpose operation. The matrix \tilde{Q} is given as

$$\tilde{Q}_{ij}(p) = \delta_{ij} - \int_{S_{ij}}^{R_{ij}} dr \epsilon^{ipr} Q_{ij}(r) \quad (95)$$

where δ_{ij} is the Kronecker delta, and

$$S_{ij} = a_i - a_j \quad (96)$$

$$R_{ij} = a_i + a_j \quad (97)$$

$$Q_{ij}(r) = 2\pi(n_i n_j)^{1/2} q_{ij}(r) \quad (98)$$

The functions $Q_{ij}(r)$ and $q_{ij}(r)$ are only nonzero over the range $S_{ij} \leq r \leq R_{ij}$. The solution for $q_{ij}(r)$ is given in [28] as

$$q_{ij}(r) = A_i \frac{r^2}{2} + B_i r + D_{ij} \quad (99)$$

$$A_i = \frac{1 - \xi_3 + 6a_i \xi_2}{(1 - \xi_3)^2} \quad (100)$$

$$B_i = -\frac{6a_i^2 \xi_2}{(1 - \xi_3)^2} \quad (101)$$

$$D_{ij} = -A_i \frac{R_{ij}^2}{2} - B_i R_{ij} \quad (102)$$

$$\xi_\alpha = \frac{\pi}{6} \sum_{j=1}^L n_j (2a_j)^\alpha \quad (103)$$

$$\alpha = 1, 2, 3$$

The computation can be carried out as follows: By using (96)–(99), $Q_{ij}(r)$ for $S_{ij} \leq r \leq R_{ij}$ can be evaluated. Then, $\tilde{Q}_{ij}(p)$ is calculated by using (95). Next, the matrix $\tilde{C}(p)$ is computed using (94). Finally, the matrix equation (93) is solved for $\tilde{H}(p)$ and pair distribution functions are calculated by inverse Fourier transformation.

References

1. Tatarskii, V. I., *Wave Propagation in a Turbulent Medium*, McGraw-Hill, New York, 1961.
2. Tsang, L., and J. A. Kong, "Microwave remote sensing of a two-layer random medium," *IEEE Transactions on Antennas And Propagation*, AP-24, 283–287, 1976.
3. Tsang, L., and J. A. Kong, "Wave theory for microwave remote sensing of a half-space random medium with three-dimensional variation," *Radio Science*, Vol. 14, 359–369, 1979.
4. Ishimaru, A., *Wave Propagation and Scattering in Random Media. Vol. I: Single Scattering and Transport Theory*. Academic Press, New York, 1978.
5. Zuniga, M. A., T. M. Habashy, and J. A. Kong, "Active remote sensing of a layered random media," *IEEE Trans. Geosci. Remote Sensing*, GE-17, No. 4, 296–302, 1979.
6. Zuniga, M., and J. A. Kong, "Active remote sensing of random media," *Journal of Applied Physics*, Vol. 51, No. 1, 74–79, 1980.
7. Tsang, L., J. A. Kong, and R. W. Newton, "Application of Strong Fluctuation random medium theory to scattering of electromagnetic waves from a vegetation-like half space," *IEEE Trans. Geosci. Remote Sensing*, GE-19, No. 1, 62–69, 1981.
8. Tsang, L., J. A. Kong, and R. T. Shin, *Theory of Microwave Remote Sensing*, John Wiley and Sons, New York, 1985.
9. Nghiem, S. V., "Electromagnetic wave models for polarimetric remote sensing of geophysical media," *Ph.D. Thesis*, Department of EECS, Massachusetts Institute of Technology, Cambridge MA, 1991.
10. McQuarrie, D. A., *Statistical Mechanics*, Harper and Row, New York, 1976.
11. Waseda, Y., *The Structure of Non-Crystalline Materials, Liquids and Amorphous Solids*, McGraw-Hill, New York, 1980.
12. Karal, F. C., and J. B. Keller, "Elastic, electromagnetic, and other waves in a random medium," *Journal of Mathematical Physics*, No. 5, 537–547, 1964.
13. Tsang, L., and J. A. Kong, "Scattering of electromagnetic waves from random media with strong permittivity fluctuations," *Radio Science*, Vol. 16, 303–320, 1981.

14. Stogryn, A., "Correlation functions for random granular media in strong fluctuation theory," *IEEE Transactions on Geoscience and Remote Sensing*, Vol. 22, No. 2, 1984.
15. Keller, J. B., "Wave propagation in random media," *Proceedings of Symposia in Applied Mathematics*, American Mathematical Society, Vol. 13, 227–246, 1962.
16. Frisch, U., "Wave propagation in Random Medium," in *Probabilistic Methods in Applied Mathematics*, edited by A. T. Bharucha-Reid, Vol. 1, 75–198, Academic, New York, 1968.
17. Stogryn, A., "Electromagnetic scattering by random dielectric constant fluctuations in a bounded medium," *Radio Science*, Vol. 9, 509–518, 1974.
18. Debye, P., H. R. Anderson, Jr., and H. Brumberger, "Scattering by an Inhomogeneous Solid.II. The Correlation Function and Its Application," *Journal of Applied Physics* Vol. 28, No. 6, 679–683, 1957.
19. Torquato, S., and G. Stell, "Microstructure of two-phase random media—III: The n-point matrix probability functions for fully penetrable spheres," *Journal of Chemical Physics*, Vol. 79, No. 3, 1983.
20. Torquato, S., and G. Stell, "Microstructure of two-phase random media.V. The n-point matrix probability functions for impenetrable spheres," *Journal of Chemical Physics*, Vol. 82, 980–987, 1985.
21. Lim, H. H., M. E. Veysoglu, S. H. Yueh, R. T. Shin, and J. A. Kong, "Random medium model approach to scattering from a random collection of discrete scatterers," *Journal of Electromagnetic Waves and Applications*, Vol. 8, 801–817, 1994.
22. Nghiem, S. V., J. A. Kong, and R. T. Shin, "Study of polarimetric response of sea ice with layered random medium model," *IGARSS Proceeding*, Vol. 3, 1875–1878, 1990.
23. Borgeaud, M., R. T. Shin, and J. A. Kong, "Theoretical models for polarimetric radar clutter," *Journal of Electromagnetic Waves and Applications*, Vol. 1, No. 1, 73–89, 1987.
24. Jin, Y. Q., and J. A. Kong, "Strong fluctuation theory for electromagnetic wave scattering by a layer of random discrete scatterers," *Journal of Applied Physics*, Vol. 55, No. 5, 1364–1369, 1984.

25. Tsang, L., J. A. Kong, and R. W. Newton, "Application of strong fluctuation random medium theory to scattering of electromagnetic waves from a halfspace of dielectric mixture," *IEEE Transactions on Antennas and Propagation*, AP-30-2, 292–302, 1982.
26. Vallese, F., and J. K. Kong, "Correlation function studies for snow and ice," *Journal of Applied Physics*, Vol. 52, 4921–4925, 1981.
27. Perovich, D. K., and A. J. Gow, "A statistical description of microstructure of young ice," *J. Geophys. Res.*, Vol. 96, No. C9, 16943–16953, 1991.
28. Baxter, R. J., "Ornstein-Zernike relation and Percus-Yevick approximation for fluid mixtures," *J. Chem. Phys.*, Vol. 52, 4559–4562, 1970.
29. Ding, K. H., and L. Tsang, "Effective propagation constants in media with densely distributed dielectric particles of multiple sizes and permittivities," *Progress in Electromagnetics Research*, PIER 1, 241–295, 1989.
30. Lebowitz, J. L., "Exact solution of generalized Percus-Yevick equation for a mixture of hard spheres," *Phys. Rev.*, Vol. 133, A895–899, 1964.
31. Wertheim, M. S., "Analytic solution of the Percus-Yevick equation," *J. Math. Phys.*, Vol. 5, 643–651, 1964.